Computational and Structural Biotechnology Journal 21 (2023) 1550–1556

Contents lists available at ScienceDirect

Computational and Structural Biotechnology Journal

journal homepage: www.elsevier.com/locate/csbj

# *Bacillus subtilis* spores displaying RBD domain of SARS-CoV-2 spike protein

A. Vetráková [1], R. Kalianková Chovanová [1], R. Rechtoríková, D. Krajčíková, I. Barák *

*Department of Microbial Genetics, Institute of Molecular Biology, Slovak Academy of Sciences, Bratislava, Slovakia*

ARTICLE INFO

*Article history:*
Received 14 November 2022
Received in revised form 16 January 2023
Accepted 4 February 2023
Available online 8 February 2023

*Keywords:*
*Bacillus subtilis*
Spore surface display
CotZ
CotY
RBD

ABSTRACT

*Bacillus subtilis* spores are considered to be efficient and useful vehicles for the surface display and delivery of heterologous proteins. In this study, we prepared recombinant spores with the receptor binding domain (RBD) of the SARS-CoV-2 spike glycoprotein displayed on their surface in fusion with the CotZ or CotY spore coat proteins as a possible tool for the development of an oral vaccine against the SARS-CoV-2 virus. The RBD was attached to the N-terminus or C-terminus of the coat proteins. We also directly adsorbed non-recombinantly produced RBD to the spore surface. SDS-PAGE, western blot and fluorescence microscopy were used to analyze RBD surface expression on purified spores. Results obtained from both display systems, recombinant and non-recombinant, demonstrated that RBD was present on the spore surfaces.

© 2023 The Authors. Published by Elsevier B.V. on behalf of Research Network of Computational and Structural Biotechnology. This is an open access article under the CC BY-NC-ND license (http://creativecommons.org/licenses/by-nc-nd/4.0/).

## 1. Introduction

*B. subtilis* is a Gram-positive bacterium commonly used for recombinant protein expression. Its spores are considered to be efficient vehicles for the surface display and delivery of heterologous proteins [1–3]. *B. subtilis* spore surface display has many advantages, including the relatively easy modification of the spore structure using genetic tools. The spores are extremely resilient and stable and can withstand extremes of temperature, desiccation, freezing, and thawing as well as exposure to solvents and other noxious chemicals, which contributes to the overall stability of the expressed and displayed heterologous proteins [4,5].

The spore-based approach also has some advantages over other microbial display systems, such as the high stability and activity of hybrid proteins in various environments, and the ability to display large multimeric proteins [6,7]. Several factors can affect the efficiency of spore surface display, including the utilization of appropriate anchor and target proteins, the use of peptide linkers, expression vectors, and other experimental parameters [7].

Both recombinant and non-recombinant approaches can be used to display heterologous proteins on the spore surface [8,9]. The recombinant method relies on the genetic modification of the bacterial genome to express a target protein in fusion with a spore coat protein [10,11]. In the non-recombinant approach, the direct adsorption of exogenous proteins to the spore surface is performed, sometimes accompanied by linkage with a cross-linking agent [8,12].

*B. subtilis* spores are surrounded by a structurally complex protein shell, known as the coat, which is organized into four major layers, from the outermost to the innermost they are crust, outer coat, inner coat and basement layer [13]. Six proteins, CotV, CotW, CotX, CotY, CotZ, and CgeA were identified in the spore crust. CotY and CotZ are distributed evenly on the spore surface, in contrast to CotX and CotV which are preferentially distributed at the spore poles [14]. The localization and abundance of the CotZ and CotY proteins make them a suitable anchor for the spore surface display technique.

Due to the unique resistance properties of spores, including their ability to survive in extreme environments such as the gastrointestinal tract, they are considered an attractive tool for delivering heterologous antigens in the form of orally administered vaccines [11,15,16]. Several studies confirm that spores used as carriers of a specific antigen can elicit an immune response, which is needed for long-lasting immunity [11,17–20].

The advantages of the spore surface display of antigens might be exploited in the fight against the SARS-CoV-2 virus which has taken millions of lives and significantly affected the global economy [21]. Companies and academic institutions have developed efficient vaccines against SARS-CoV-2, which can control the spread of the disease and decrease the death toll of infected people [22]. The majority of the approved COVID-19 vaccines rely on the spike protein (S) of SARS-CoV-2, since antibodies targeting the S protein block the entry

* Corresponding author.
*E-mail address:* imrich.barak@savba.sk (I. Barák).
[1] Equal contribution

https://doi.org/10.1016/j.csbj.2023.02.007
2001-0370/© 2023 The Authors. Published by Elsevier B.V. on behalf of Research Network of Computational and Structural Biotechnology. This is an open access article under the CC BY-NC-ND license (http://creativecommons.org/licenses/by-nc-nd/4.0/).

**Table 1**
Strain list.

| Strains | Description | Source of reference |
|---|---|---|
| *Bacillus subtilis* | | |
| PY79 | type strain | [30] |
| IB1816 | amyE::*cotZ*-linker-spike glycoprotein RBD | This work |
| IB1817 | amyE:: spike glycoprotein RBD-linker-*cotZ* | This work |
| IB1818 | amyE::*cotY*-linker-spike glycoprotein RBD | This work |
| IB1819 | amyE:: spike glycoprotein RBD-linker-*cotY* | This work |
| *Escherichia coli* | | |
| DH5α | type strain | Laboratory stock |
| BL21 (DE3) | type strain | Laboratory stock |
| Plasmids | | |
| pGBWm4046887 | Plasmid for SARS-CoV-2 surface glycoprotein | Addgene |
| pDG1662 | Cloning vector for ectopic integration | [38] |
| pET28a | Vector for bacterial expression | Novagen |

of the virus into the target cells and thus, prevent the virus from replicating [23].

The multifunctional, homotrimeric S protein is cleaved by one of the host proteases (e. g. cellular serine protease TMPRSS2, furin) into two functionally distinct subunits – the membrane-distal S1 subunit, and the membrane-proximal S2 subunit. The S1 subunit contains a receptor binding domain (RBD), which binds specifically to the angiotensin-converting enzyme (ACE-2) of a target cell [24,25] and thereby induces the necessary conformational changes which initiate the fusion of viral and host membranes, which is driven by the S2 subunit. The S2 subunit contains segments that are essential for facilitating these processes, and are highly conserved among the coronavirus family. The S1 subunit is highly diverse due to the use of different receptors in different hosts [26,27]. Some pharmaceutical companies have developed vaccines based on the use of the full-length S glycoprotein, but some vaccine candidates solely rely on the highly immunogenic RBD subunit, which elicits good quality, highly specific antibodies [11,28].

Herein, we displayed the SARS-CoV-2 spike glycoprotein RBD on the surface of *B. subtilis* spores using CotZ or CotY as fusion anchors. RBD was attached to the N-terminus or C-terminus of both spore coat proteins and we demonstrated that all four types of hybrid proteins were successfully displayed on the spore surface. Using immunofluorescence microscopy, we also confirmed the direct adsorption of the RBD recombinant protein on the spore surface.

## 2. Materials and methods

### 2.1. Bacterial strains

*Escherichia coli* strain DH5$\alpha$ (F− 80dlacZ M15 (supE44 Δ(lacZYA-argF)U196 (Φ80ΔlacZM15) hsdR17 recA1endA1 gyrA96 thi-1 relA1) [29] was chosen as the host for the cloning and maintenance of all plasmids. For expression and purification of RBD *E. coli* strain BL21 (DE3) (F–, *ompT, hsdSB, (rB–mB–), gal, dcm*) (Novagen®, Merck KGaA, Darmstadt, Germany) was used. The genomic DNA of *Bacillus subtilis* wild strain PY79 [30] was used for the amplification of genes encoding the spore coat proteins CotZ and CotY. Recombinant strains containing the CotZ-RBD, RBD-CotZ, CotY-RBD, and RBD-CotY fusions are all isogenic derivatives of *B. subtilis* PY79. Bacteria were grown in LB medium supplemented with appropriate antibiotics at 37 °C. The bacterial strains together with the plasmids used in this study are listed in Table 1.

### 2.2. Construction of strains carrying coat protein – RBD fusion

Four recombinant strains harboring the RBD-coat protein fusions were prepared, and the RBD domain was placed either on the N-terminus or C-terminus of the coat protein. *B. subtilis* chromosome integration vector pDG1662 was used and plasmids were constructed by Gibson assembly [31]. DNA fragments encoding for coat protein genes were PCR amplified using the *B. subtilis* PY79 genomic DNA as a template and the oligonucleotides listed in Table 2. The spike glycoprotein *rbd* gene was amplified by PCR from the pGBWm4046887 plasmid (Addgene plasmid No. 145730). In all PCR reactions Phusion ® High-Fidelity DNA Polymerase was used according to the standard guidline (https://lnk.sk/fpzd).

Plasmid pDGCotZ-RBD, with the RBD protein on the C-terminus of CotZ, was constructed using a 250-bp $P_{cotYZ}$ promoter region amplified with primers PcotYZ_47F and PcotYZ_*cotZ*CL_R; the 441-bp *cotZ* gene was amplified with the *cotZ*_CL_F and *cotZ*_CL_R primers and the 805-bp SARS-CoV-2 spike glycoprotein *rbd* gene was amplified with the RBD_*cotZ*_CL_F and RBD_*cotZ*CL_R primers. PCR fragments were inserted into a pDG1662 plasmid that had previously been cleaved with the *Bam*HI and *Eco*RI restriction enzymes.

To construct plasmid pDGRBD-CotZ, which carries the RBD region of the spike protein on the N-terminus of CotZ, we prepared 3 PCR fragments: a 250-bp DNA fragment of the $P_{cotYZ}$ promoter region, which was amplified by PCR with the PcotYZ_47F and PcotYZ_NL_R primers; an 805-bp fragment corresponding to the SARS-CoV-2 spike glycoprotein *rbd* gene amplified with primers RBD_NL_F and RBD_NL_R; and a 441-bp *cotZ* gene amplified with primers *cotZ*_NL_F and *cotZ*_NL_R. PCR fragments were inserted into a pDG1662 plasmid which had been previously cleaved with *Bam*HI and *Eco*RI.

Plasmid pDGCotY-RBD for the C-terminal fusion of CotY and RBD was constructed using two PCR fragments: a 729-bp fragment containing the *cotY* gene and its upstream sequence, including the promoter region, was amplified with the PcotYZ_65F and PcotYZ_*cotY*_CL_R oligonucleotides and an 805-bp PCR fragment containing the SARS-CoV-2 spike glycoprotein *rbd* gene, amplified with RBD_*cotY*_CL_F and RBD_*cotY*_CL_R. These fragments were inserted into a pDG1662 plasmid which had been previously cleaved with *Bam*HI and *Eco*RI.

Plasmid pDGRBD-CotY was prepared by the insertion of three PCR fragments into a pDG1662 plasmid which had been previously cleaved with *Bam*HI and *Eco*RI: a 250-bp DNA fragment of the promoter region amplified by PCR using the PcotYZ_65F and PcotYZ_*cotY*_NL_R oligonucleotides; an 805-bp PCR fragment corresponding to the SARS-CoV-2 spike glycoprotein *rbd* gene, amplified by PCR using the RBD_NL_F and RBD_NL_R primers and a 486-bp fragment containing the *cotY* gene, amplified with *cotY*_NL_F and *cotY*_NL_R. All cloned sequences were confirmed by DNA sequencing.

*B. subtilis* competent cells were transformed with recombinant plasmids and the clones generated after the integration of the cloned DNA at the *amyE* (amylase) locus of *B. subtilis* were selected on agar plates supplemented with 5 μg/ml chloramphenicol.

**Table 2**
List of PCR oligonucleotides.

| Name | Sequence |
|---|---|
| PcotYZ_47F | AAATTAAAAACTGGTCTGATCGGACAGCAACAAATACACTCGTAGCC |
| PcotYZ_*cotZ*CL_R | CTTGATGTTTTCTGGCTCATGATTTCAGCTCCTTCTTTATAGG |
| *cotZ*_CL_F | ATAAAGAAGGAGCTGAAATCATGAGCCAGAAAACATCAAG |
| *cotZ*_CL_R | TTAGGTCTTGGTGGTGGTGGATGATGATGTGTACGATTGATTAA |
| RBD_*cotZ*_CL_F | ATCATCCACCACCACCAAGACCTAATATTACAAACTTGTGCCC |
| RBD_*cotZ*_CL_R | GATAAGCTGTCAAACATGAGTTACTCAAGTGTCTGTGGATCACGGAC |
| PcotYZ_NL_R | AAGTTTGTAATATTAGGCATGATTTCAGCTCCTTCTTTATAGG |
| RBD_NL_F | ATAAAGAAGGAGCTGAAATCATGCCTAATATTACAAACTTGTGC |
| RBD_NL_R | CTCATTCTTGGTGGTGGTGGCTCAAGTGTCTGTGGATCAC |
| *cotZ*_NL_F | TTGAGCCACCACCACCAAGAATGAGCCAGAAAACATCAAG |
| *cotZ*_NL_R | GATAAGCTGTCAAACATGAGTTAATGATGATGTGTACGATTGATTAATCGAGGATTTAAGC |
| PcotYZ_65F | GGACACATGGAAACACACAAATTAAAAACTGGTCTGATCGGACAGCAACAAATACACTCGTAGCC |
| PcotYZ_*cotY*_CL_R | TTAGGTCTTGGTGGTGGTGGTCCATTGTGATGATGCTTTTT |
| RBD_*cotZY*_CL_F | ATGGACCACCACCACCAAGACCTAATATTACAAACTTGTGCCC |
| RBD_*cotY*_CL_R | TAAGGGTAACTATTGCCGATGATAAGCTGTCAAACATGAGTTACTCAAGTGTCTGTGGATCACGGAC |
| PcotYZ_*cotY*_NL_R | AAGTTTGTAATATTAGGCATGATTTCAGCTCCTTCTTTATAGGGTATTTGACT |
| RBD_NL_F | ATAAAGAAGGAGCTGAAATCATGCCTAATATTACAAACTTGTGC |
| RBD_NL_R | CTCATTCTTGGTGGTGGTGGCTCAAGTGTCTGTGGATCAC |
| *cotY*_NL_F | TTGAGCCACCACCACCAAGAATGAGCTGCGGAAAAACCCA |
| *cotY*_NL_R | GCCGATGATAAGCTGTCAAACATGAGTTATCCATTGTGATGATGCTTTTTATC |
| Spike_RBD_F | ACCGGATCCCCTAATATTACAAACTTGTGCC |
| Spike_RBD_R | ACCCTCGAGTTAATGATGATGTGTACGATTG |

### 2.3. Expression and purification of the receptor binding domain (RBD)

To express the SARS-CoV-2 spike glycoprotein RBD, we used expression plasmid pET28a. The *rbd*, part of the SARS-CoV-2 spike gene, was amplified with specific primers (Table 2) from plasmid pGBWm4046887 and, after cleavage with the *Bam*HI and *Xho*I restriction enzymes, cloned into the corresponding cloning site of a pET28a plasmid. *E. coli* BL21 (DE3) competent cells were transformed with the expression plasmid pET28RBD and grown in LB medium supplemented with kanamycin at 16 °C until $OD_{600}$ ≈ 0.6. Protein expression was induced by the addition of 1 mM isopropyl-β-D-1-thiogalactopyranoside (IPTG). The cells were collected after overnight cultivation at 16 °C and stored at − 80 °C until used. To isolate the protein, bacteria were lysed by sonication and the lysate was centrifuged at 73,000g for 30 min. After centrifugation of the crude cell lysate, the protein was purified using a 1 ml Ni-column. Because we found that the RBD protein produced in *E. coli* was mostly insoluble, we supplemented the 50 mM Tris/HCl solubilization buffer, pH 9.0, containing 150 mM NaCl with 8 M urea.

### 2.4. Preparation of spores

The sporulation of wild-type PY79 and recombinant strains was induced by the exhaustion method in Difco sporulation medium (DSM) [32]. A single colony was used to inoculate LB medium and cultivated overnight at 37 °C. This culture was then used to inoculate liquid LB and the bacteria were grown until $OD_{600}$ ≈ 1.0. Subsequently, 200 μl of this culture was spread on DSM plates and left at 37 °C for 3 days, followed by growth at room temperature for another 3 days. Spores were harvested and purified by intensive washing with ice-cold water for at least a week to remove cell debris and vegetative cells, after which spores were washed at least twice a week, and stored at 4 °C until use.

### 2.5. Adsorption reaction

The RBD protein was purified using a buffer containing 8 M urea. To obtain native, non-denatured protein, the urea was removed using a centrifugal concentrator (Amicon® ultra-4 centrifugal filter unit). For the adsorption reaction, 4 μg of RBD was added to a suspension of $2 \times 10^9$ *B. subtilis* WT PY79 spores in 0.15 M PBS buffer pH 4.0. After one hour of incubation at room temperature, the spores were centrifuged for 10 min at 13,000g. The pellet was then resuspended in 0.15 M PBS pH 4.0 and stored at 4 °C for further experiments [33].

### 2.6. Expression of fusion proteins in B. subtilis and western blot analysis

To analyze the expression level of the fusion proteins in sporulating *B. subtilis* cells, we used the western blot technique. Bacterial samples were collected at different time points after the onset of sporulation. Cell aliquots at $OD_{600}$ ≈ 40 (a bacterial culture with $OD_{600}$ ≈ 3.5 contained approx. $4 \times 10^8$ CFU) were suspended in solubilization buffer (50 mM Tris/HCl, pH 9.0, 150 mM NaCl, 0.4 mg/ml lysosome, cOmplete Protease Inhibitor Cocktail (Sigma-Aldrich)), and incubated at 37 °C for 20 min. After sonication lysates were treated with SDS buffer (62.5 mM Tris-HCl pH 6.8, 4% SDS, 5% glycerol, 2% β-mercaptoethanol, 0.003% bromophenol blue) for 10 min at 95 °C. Proteins were resolved by SDS-PAGE electrophoresis and subsequently analyzed by western blot analysis using a mouse monoclonal antibody against RBD protein (Abcam ab277628).

### 2.7. Immunofluorescence microscopy

Spores were collected and used for immunofluorescence microscopy as described by Harry et al. [34] with the following modifications. Spores were blocked with 2% bovine serum albumin in PBS for 20 min at room temperature. Subsequently, samples were incubated overnight at 4 °C with the mouse anti-SARS-CoV-2 Spike Glycoprotein RBD antibody at a dilution 1:1000. Samples were then washed three times in PBS and incubated for two hours with the Alexa Fluor 594 labelled anti-mouse IgG (ThermoFisher, A11005) at room temperature in the dark at a dilution 1:500. Samples were washed three times in PBS and, subsequently, 1 μl was applied on a glass slide, and the sample was then observed and photographed with an Olympus BX63 microscope equipped with an Andor Zyla 5.5 sCMOS camera (Olympus Europa SE & Co. KG., Hamburg, Germany). Olympus CellP imaging software was used for image acquisition and analysis. The final adjustment of the fluorescent images was done using Fiji ImageJ (open-source software).

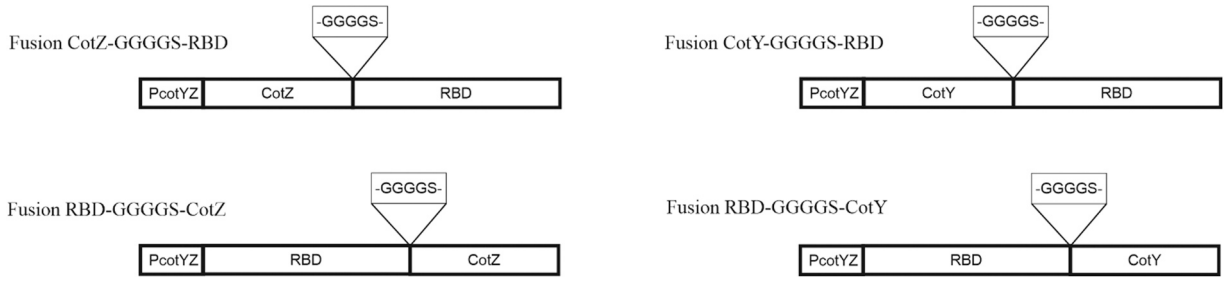


**Fig. 1.** Schematic representation of fusion proteins for spore display. Construction of four fusions carrying the genes of both hybrid variants, the N-terminal and C-terminal fusion of coat protein CotZ or CotY to RBD. Fusion protein expression was controlled by the native $P_{cotYZ}$ promoter. The flexible peptide linker GGGGS was inserted between the coat protein and RBD.

### *2.8. Modelling of 3D structure of CotY-RBD*

The three-dimensional reconstruction of CotY crystals is adapted from Jiang et al. [35]. The monomer structure of the CotY protein was predicted using AlphaFold [36,37]. The SARS-CoV-2 spike glycoprotein RBD protein structure was adapted from Protein Data Bank structure 6M0J.

## 3. Results and discussion

*B. subtilis* is widely used for the expression and spore surface display of heterologous proteins by integrating the target gene into the *B. subtilis* chromosome [2,39]. In this study, we intended to develop an alternative strategy for preparing potential vaccines against the SARS-CoV-2 virus in large quantities and with an easy route of administration. Our goal was to prepare recombinant spores with the RBD region of the SARS-CoV-2 spike protein displayed on their surface and to examine whether we would be able to detect the attached protein. Meanwhile, another study was published that focused on preparing recombinant spores which anchored the RBD to the outer coat proteins CotA, CotB and CotC [11]. This study showed that the expression of the CotC-linked RBD in *B. subtilis* cells was much higher, while the CotA and CotB-linked RBD was not detectable. Significant increases in the level of antibody against sRBD in both mice and humans were reported after the oral administration of spores carrying the hybrid protein CotC-RBD.

In this study, we used CotY and CotZ as the anchor proteins for the spore display of RBD. In contrast to the other coat proteins used, especially CotB, CotC, and CotG which are widely exploited as a platform for the display of various proteins, CotY and CotZ have only been used in a few cases [2]. Since they are located closer to the spore surface, they provide a strong signal in immunofluorescent microscopy [14,40]. CotY and CotZ were proposed to be good candidates for the attachment of foreign proteins and their efficient display on the spore surface. For the target protein, we used a fragment containing residues 330–583 of the receptor-binding domain (RBD) of the spike protein, which is crucial in the process of cell invasion by the virus [23,26,41].

### *3.1. Construction of recombinant B. subtilis spores*

To obtain recombinant *B. subtilis* spores displaying the SARS-CoV-2 spike glycoprotein RBD on their surface, we prepared four integrative plasmids carrying genes for two variants in which the RBD was fused to either the N-terminus or the C-terminus of the coat protein. Fusion protein production was controlled by the native $P_{cotYZ}$ promoter to ensure the proper timing of expression during the formation of the spore coat. We also inserted the flexible peptide linker GGGGS between the coat protein and the RBD (Fig. 1). All gene fusions were integrated into the coding sequence of the non-essential *amyE* locus of the *B. subtilis* chromosome and the correct clones were selected by chloramphenicol resistance. All recombinant strains were used for further analysis. The recombinant strains and their isogenic parental strain PY79 showed comparable sporulation efficiency, indicating that the presence of the fusion did not significantly affect sporulation efficiency.

### *3.2. Expression of fusion genes and western blot analysis*

Next, we analyzed the production of hybrid proteins during sporulation. Proteins from the *B. subtilis* PY79 wild-type, CotZ-RBD, RBD-CotZ, CotY-RBD, and RBD-CotY strains were fractionated in 10% polyacrylamide gels containing SDS. The protein lysates obtained from the 2nd, 4th, 6th, 8th and 24th hours of sporulation were analyzed. An equal amount of cells corresponding to an $OD_{600} \approx 40$ was taken for analysis. As the time after the onset of sporulation increased, we could observe a gradual decrease in the amount of proteins in the SDS gels (Fig. 2) which corresponds to an increased proportion of spores in the cell culture and the lower solubility of the spore coat proteins compared to the proteins of vegetative cells. To test the expression level of the fusion genes, we performed a western blot analysis with the anti-SARS-CoV-2 spike glycoprotein RBD antibody. The pattern obtained from the recombinant strains varies significantly (Fig. 2), but in contrast to the wild-type, which served as a control and did produced no western blot signal (Fig. 2F), RBD signals are present in all recombinant strains 4 and 6 h after the onset of sporulation. Furthermore, we observed that the fusion proteins were rather degraded, but several bands corresponding to higher molecular weights were observed, most likely representing oligomerized forms of the hybrid proteins. The C-terminal fusion of CotZ and RBD resulted in the formation of large oligomers but at hours 8 and 24 these signals were lost. We assume that the hybrid CotZ-RBD was incorporated into the spore coat as part of the insoluble spore coat structure that cannot be solubilized using the common techniques [42], and thus, we were not able to detect them by western blotting. When RBD was attached to the N-terminus of CotZ, we did not see any bands corresponding to the larger proteins, suggesting that this arrangement could preclude the formation of CotZ-RBD oligomers. When RBD was attached to the N-terminus of CotY, in addition to the strong signals representing degradation products, a weak band corresponding to the high molecular weight oligomers characteristic of the CotY protein itself was detected on the SDS-PAGE gel. Using ImageJ (open-source software), we calculated that this macro structure represents at least 3% of the hybrid RBD-CotY protein. In contrast, the C-terminal fusion of CotY and RBD produced a wide range of signal sizes, even some with high molecular weight, but without the typical CotY pattern, which is characterized by the existence of discrete bands corresponding to high molecular weight oligomers at the top of the SDS gel [35]. These bands appear to be the result of adsorption of aggregated and/or degraded fusion protein on the spore surface. We hypothesize that the fusion protein was not incorporated into CotY structures: even

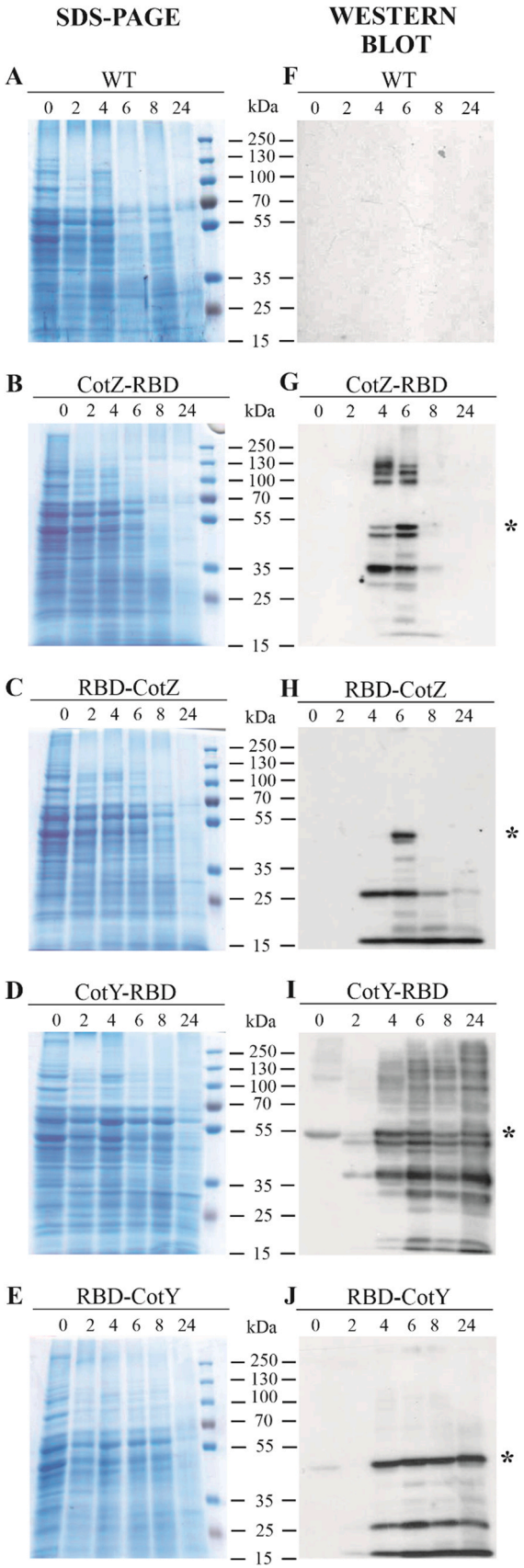


**Fig. 2.** SDS-PAGE and western blot analysis of proteins extracted from spores of the *B. subtilis* wild-type (WT) strain and recombinant strains CotZ-RBD, RBD-CotZ, CotY-RBD, and RBD-CotY at different sporulation times. Cell lysates (cell cultures with $OD_{600}$ ≈ 3.5 contained approx. $4 \times 10^8$ CFU and an aliquot of $OD_{600}$ ≈ 40 was used) were resolved on 10% SDS polyacrylamide gels (A-E). Fractionated proteins were subsequently transferred onto a nitrocellulose membrane and probed with a monoclonal antibody against the RBD protein (F-J). Cells from the onset of sporulation (lane 0) and the 2nd (lane 2), 4th (lane 4), 6th (lane 6), 8th (lane 8), and 24th (lane 24) hours of sporulation were analyzed. Molecular weight markers (in kilodaltons) are indicated. Stars mark the size of the fused proteins.

after the 24 h of sporulation, when the total amount of solubilized protein is low, we observed a strong signal corresponding to the RBD protein which most likely resulted from the adsorption of RBD and which could be more easily released into solubilization buffer. Western blot analysis of intensively washed spores did not show any large oligomers of RBD-containing fusion proteins, only some digestion products. We hypothesize that if hybrid proteins form the structures with the intrinsic coat proteins, they will become part of the coat fraction that cannot be easily solubilized. We also do not anticipate that there would be a large number of hybrid protein molecules incorporated directly into the CotY or CotZ 2D crystals formed by these proteins within the spore coat [43]. Fig. 4 reflects an ideal model situation for the incorporation of the fusion protein CotY-RBD into the spore crust. However, the RBD protein is twice as big as either CotY or CotZ and we expect that there could be some steric hindrance in 2D crystal formation from these two proteins. This fact is also confirmed by the diversity of the western blot results (Fig. 2). Nevertheless, RBD is successfully displayed on the spore surface and, even when attached to the spore surface by adsorption, it is captured tightly enough that it cannot be removed by vigorous spore washing (Fig. 3A – WT-RBD).

### 3.3. Immunofluorescence microscopy

To further verify whether the SARS-CoV-2 spike glycoprotein RBD is displayed on the spore surface, we performed fluorescence immunoassays with the primary anti-SARS-CoV-2 Spike Glycoprotein RBD and Alexa Fluor 594 labelled anti-mouse IgG secondary antibodies. We observed a fluorescence signal around the recombinant spores of all fusions with a minimal fluorescence signal for wild-type *B. subtilis* spores, which might arise from the direct adsorption of antibodies onto the spore surface (Fig. 3A). The C-terminal fusion of CotZ with RBD appears to be the optimal arrangement; this is consistent with the results of western blot analysis, which showed that a significant portion of the fusion protein was not degraded and was probably incorporated into the coat structure. The immunoreactivity of both CotY fusions seems to be similar, although we suggest, based on the results of the western blotting, that the incorporation of the fusion protein should proceed better for the N-terminal RBD-CotY fusion. The C-terminal fusion protein was probably adsorbed onto the spore surface during spore coat formation in the bacterial cytoplasm. Obviously, as reviewed by Ricca et al. [44], this strategy is effective for most antigens. Our experiment with the adsorption of the RBD protein alone onto spores (Fig. 3A – WT-RBD) showed that this approach is effective. The immunofluorescence microscopy results of both the recombinant spores and spores with RBD adsorbed, demonstrate that the SARS-CoV-2 spike glycoprotein RBD was available for antibody binding. Furthermore, we used data from immunofluorescence microscopy to compare fluorescence intensity using ImageJ. The fluorescence intensity of spores with RBD adsorbed on the surface is markedly higher than those of the recombinant strains. While it is possible that the adsorbed proteins might infiltrate into the coat layers [45], we hypothesize that this phenomenon might arise because the adsorbed proteins are not embedded into the spore surface and may, therefore, be more accessible to the primary antibody (Fig. 3B).

When considering whether recombinant *B. subtilis* spores displaying the RBD-CotY and/or RBD-CotZ fusion proteins would be suitable for oral vaccine development, several factors speak in their favor. First, *B. subtilis* is considered GRAS (generally regarded as safe)

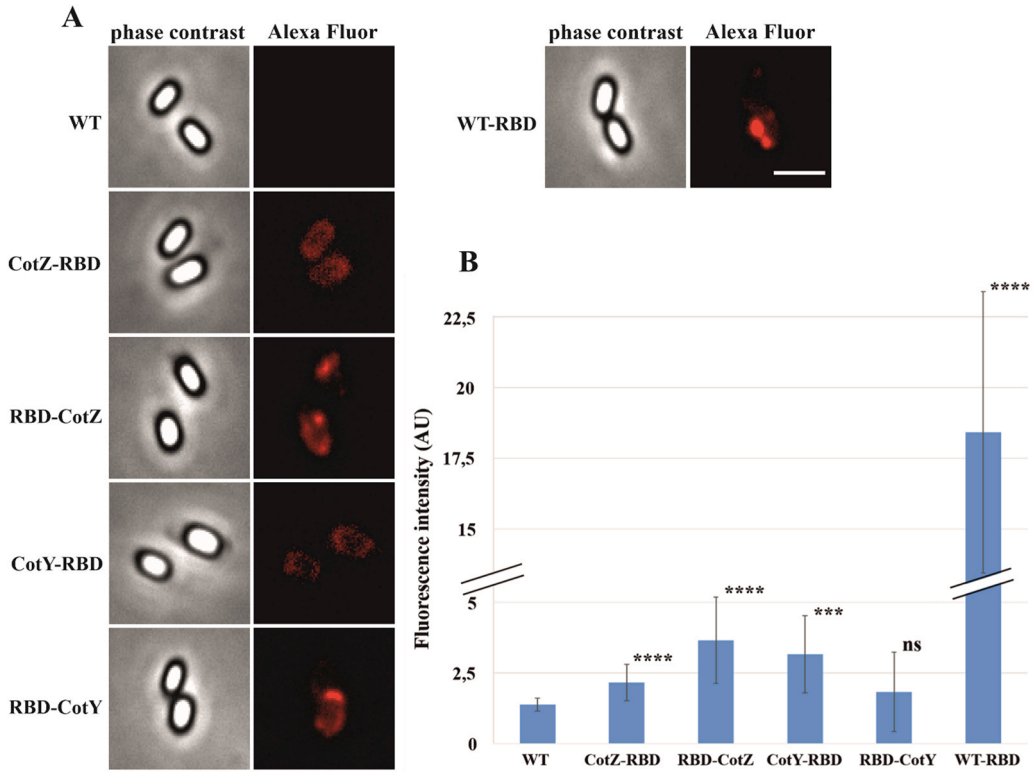


**Fig. 3.** Immunofluorescence microscopy of the *B. subtilis* PY79 wild-type spores, recombinant derivatives and spores with the SARS-CoV-2 spike glycoprotein RBD adsorbed on the surface and their fluorescence intensity. A: The left panel shows phase contrast images of wild-type strain PY79, CotZ-RBD, RBD-CotZ, CotY-RBD, RBD-CotY and WT-RBD and immunofluorescence microscopy images are shown in the right panel. The spores were incubated with the mouse anti-SARS-CoV-2 Spike Glycoprotein RBD antibody, followed by an incubation with the anti-mouse IgG- Alexa Fluor 594 conjugate. The scale bar represents 2 µm. B: Fluorescence intensity quantification of recombinant strains and spores with the SARS-CoV-2 spike glycoprotein RBD adsorbed on the surface compared to WT using ImageJ software. Significant p-values between WT and the recombinant samples from two-tailed unpaired t-tests are depicted above the plot; the threshold for statistical significance is as follows: stars indicate significantly different values, where ns (not significant) corresponds to p-value > 0.05, * to $p \leq 0.05$, ** to $p \leq 0.01$, *** to $p \leq 0.001$ and **** to $p \leq 0.0001$. The size of the sample from each strain is 16 (n = 16).

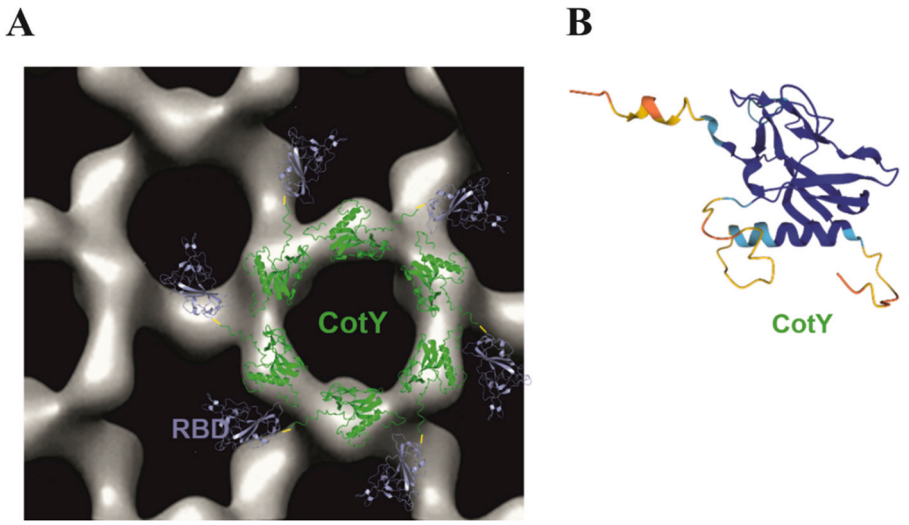


**Fig. 4.** Model of the CotY-RBD fusion protein structure. A: Three-dimensional surface representations of the 2D CotY crystal into which the predicted AlphaFold 3D structure of CotY is superimposed. The three-dimensional reconstruction of the CotY crystals is adapted from Jiang et al. [35]. The RBD domain of the SARS-CoV-2 spike protein structure is adapted from Protein DataBank structure 6M0J. B: The monomer structure of the CotY protein as predicted by AlphaFold [46]. AlphaFold produces a per-residue confidence score (pLDDT) between 0 and 100. pLDDT ≥ 90 represents very high model confidence (dark blue), while the value 90 > pLDDT ≥ 70 is classified as confident (light blue). 70 > pLDDT ≥ 50 indicates low confidence (yellow), pLDDT < 50 belongs to very low confidence (orange). Some regions with low pLDDT may be unstructured in isolation.

by the US Food and Drug Administration and is also used as a probiotic and feed additive product for humans and animals [47–49]. Spores can survive the harsh environment in the gastrointestinal tract caused by gastric acids and thus they are an ideal vehicle for the oral administration of vaccines [16,50]. Also, other studies have pointed out the benefits of using spores as vaccines. They stimulate a high immune response with a strong adjuvant effect [51] and, in addition, Hinc et al. [52] found that CotZ hybrid proteins elicited a stronger immune response than other antigens in a mouse model. Also, the inability to retrieve full-size hybrid proteins from the spore

coat, when most likely incorporated into the CotY/CotZ protein macro structures - even after using harsh solubilization conditions, suggests that the proteins are held on the spore surface very tightly. Thus, our observations imply that the RBD-CotY/CotZ recombinant spores could be considered for the future development of oral vaccines. Further experiments should determine whether these *B. subtilis* spores can stimulate an immune response and specific antibody production in mice Fig. 4.

## CRediT authorship contribution statement

**A. Vetráková:** Methodology, Investigation, Writing – original draft. **R. Kalianková Chovanová:** Methodology, Investigation, Writing – original draft. **R. Rechtoríková:** Methodology, Investigation. **D. Krajčíková:** Methodology, Supervision. **I. Barák:** Conceptualization, Investigation, Supervision, Funding acquisition.

## Acknowledgments

This work was supported by VEGA – Grant No. 2/0001/21 from the Slovak Academy of Sciences, a Grant from the Slovak Research and Development Agency under contract APVV-18–0104 to IB. We thank Jacob Bauer for critically reading the manuscript.

## Declaration of interests

The authors declare no conflict of interest.

## References

[1] Guoyan Z, Yingfeng A, Zabed HM, Qi G, Yang M, et al. *Bacillus subtilis* spore surface display technology: a review of its development and applications. J Microbiol Biotechnol 2019;29(2):179–90.
[2] Lin P, Yuan H, Du J, Liu K, Liu H, et al. Progress in research and application development of surface display technology using *Bacillus subtilis* spores. Appl Microbiol Biotechnol 2020;104(6):2319–31.
[3] Schallmey M, Singh A, Ward OP. Developments in the use of *Bacillus* species for industrial production. Can J Microbiol 2004;50(1):1–17.
[4] Henriques AO, Moran Jr. CP. Structure, assembly, and function of the spore surface layers. Annu Rev Microbiol 2007;61:555–88.
[5] Wang N, Chang C, Yao Q, Li G, Qin L, et al. Display of *Bombyx mori* alcohol dehydrogenases on the *Bacillus subtilis* spore surface to enhance enzymatic activity under adverse conditions. PLoS One 2011;6(6):e21454.
[6] Tavassoli S, Hinc K, Iwanicki A, Obuchowski M, Ahmadian G. Investigation of spore coat display of *Bacillus subtilis* β-galactosidase for developing of whole cell biocatalyst. Arch Microbiol 2013;195(3):197–202.
[7] Wang H, Wang Y, Yang R. Recent progress in *Bacillus subtilis* spore-surface display: concept, progress, and future. Appl Microbiol Biotechnol 2017;101(3):933–49.
[8] Donadio G, Lanzilli M, Sirec T, Ricca E, Isticato R. Localization of a red fluorescence protein adsorbed on wild type and mutant spores of *Bacillus subtilis*. Micro Cell Fact 2009;15(1):153.
[9] Hinc K, Isticato R, Dembek M, Karczewska J, Iwanicki A, et al. Expression and display of UreA of *Helicobacter acinonychis* on the surface of *Bacillus subtilis* spores. Micro Cell Fact 2010;9:2.
[10] Mauriello EM, Duc le H, Isticato R, Cangiano G, Hong HA, et al. Display of heterologous antigens on the *Bacillus subtilis* spore coat using CotC as a fusion partner. Vaccine 2004;22(9–10):1177–87.
[11] Sung JC, Liu Y, Wu KC, Choi MC, Ma CH, et al. Expression of SARS-CoV-2 spike protein receptor binding domain on recombinant *B. subtilis* on spore surface: a potential COVID-19 oral vaccine candidate. Vaccin (Basel) 2021;10(1):2.
[12] Ricca E, Baccigalupi L, Cangiano G, De Felice M, Isticato R. Mucosal vaccine delivery by non-recombinant spores of *Bacillus subtilis*. Micro Cell Fact 2014;13:115.
[13] Plomp M, Carroll AM, Setlow P, Malkin AJ. Architecture and assembly of the *Bacillus subtilis* spore coat. PLoS One 2014;9(9):e108560.
[14] Bartels J, Blüher A, López Castellanos S, Richter M, Günther M, et al. The *Bacillus subtilis* endospore crust: protein interaction network, architecture and glycosylation state of a potential glycoprotein layer. Mol Microbiol 2019;112(5):1576–92.
[15] Cao Y, Li Z, Yue Y, Song N, Peng L, et al. Construction and evaluation of a novel *Bacillus subtilis* spores-based enterovirus 71 vaccine. J Appl Biomed 2013;11(2):105–13.
[16] Duc LH, Hong HA, Fairweather N, Ricca E, Cutting SM. Bacterial spores as vaccine vehicles. Infect Immun 2003;71(5):2810–8.
[17] Ciabattini A, Parigi R, Isticato R, Oggioni MR, Pozzi G. Oral priming of mice by recombinant spores of *Bacillus subtilis*. Vaccine 2004;22(31–32):4139–43.
[18] Hoang TH, Hong HA, Clark GC, Titball RW, Cutting SM. Recombinant *Bacillus subtilis* expressing the *Clostridium perfringens* alpha toxoid is a candidate orally delivered vaccine against necrotic enteritis. Infect Immun 2008;76(11):5257–65.
[19] Li L, Hu X, Wu Z, Xiong S, Zhou Z, et al. Immunogenicity of self-adjuvanticity oral vaccine candidate based on use of *Bacillus subtilis* spore displaying *Schistosoma japonicum* 26 kDa GST protein. Parasitol Res 2009;105(6):1643–51.
[20] Tavares Batista M, Souza RD, Paccez JD, Luiz WB, Ferreira EL, et al. Gut adhesive *Bacillus subtilis* spores as a platform for mucosal delivery of antigens. Infect Immun 2014;82(4):1414–23.
[21] Li Q, Guan X, Wu P, Wang X, Zhou L, et al. Early transmission dynamics in Wuhan, China, of novel coronavirus-infected pneumonia. N Engl J Med 2020;382(13):1199–207.
[22] Koirala A, Joo YJ, Khatami A, Chiu C, Britton PN. Vaccines for COVID-19: the current state of play. Paediatr Respir Rev 2020;35:43–9.
[23] Martínez-Flores D, Zepeda-Cervantes J, Cruz-Reséndiz A, Aguirre-Sampieri S, Sampieri A, et al. SARS-CoV-2 vaccines based on the spike glycoprotein and implications of new viral variants. Front Immunol 2021;12:701501.
[24] Hoffmann M, Kleine-Weber H, Schroeder S, Krüger N, Herrler T, et al. SARS-CoV-2 cell entry depends on ACE2 and TMPRSS2 and Is blocked by a clinically proven protease inhibitor. Cell 2020;181(2):271–80.
[25] Meirson T, Bomze D, Markel G. Structural basis of SARS-CoV-2 spike protein induced by ACE2. Bioinformatics 2021;37(7):929–36.
[26] Walls AC, Park YJ, Tortorici MA, Wall A, McGuire AT, et al. Structure, function, and antigenicity of the SARS-CoV-2 spike glycoprotein. Cell 2020;181(2):281–92.
[27] Walls AC, Tortorici MA, Bosch BJ, Frenz B, Rottier PJM, et al. Cryo-electron microscopy structure of a coronavirus spike glycoprotein trimer. Nature 2016;531(7592):114–7.
[28] Dai L, Gao GF. Viral targets for vaccines against COVID-19. Nat Rev Immunol 2021;21(2):73–82.
[29] Woodcock DM, Crowther PJ, Doherty J, Jefferson S, DeCruz E, et al. Quantitative evaluation of *Escherichia coli* host strains for tolerance to cytosine methylation in plasmid and phage recombinants. Nucleic Acids Res 1989;17(9):3469–78.
[30] Youngman P, Perkins JB, Losick R. Construction of a cloning site near one end of Tn917 into which foreign DNA may be inserted without affecting transposition in *Bacillus subtilis* or expression of the transposon-borne erm gene. Plasmid 1984;12(1):1–9.
[31] Gibson DG, Young L, Chuang RY, Venter JC, Hutchison 3rd CA, et al. Enzymatic assembly of DNA molecules up to several hundred kilobases. Nat Methods 2009;6(5):343–5.
[32] van Ooij C, Eichenberger P, Losick R. Dynamic patterns of subcellular protein localization during spore coat morphogenesis in *Bacillus subtilis*. J Bacteriol 2004;186(14):4441–8.
[33] Isticato R, Sirec T, Treppiccione L, Maurano F, De Felice M, et al. Non-recombinant display of the B subunit of the heat labile toxin of *Escherichia coli* on wild type and mutant spores of *Bacillus subtilis*. Micro Cell Fact 2013;12:98.
[34] Harry EJ, Pogliano K, Losick R. Use of immunofluorescence to visualize cell-specific gene expression during sporulation in *Bacillus subtilis*. J Bacteriol 1995;177(12):3386–93.
[35] Jiang S, Wan Q, Krajcikova D, Tang J, Tzokov SB, et al. Diverse supramolecular structures formed by self-assembling proteins of the *Bacillus subtilis* spore coat. Mol Microbiol 2015;97(2):347–59.
[36] Jumper J, Evans R, Pritzel A, Green T, Figurnov M, et al. Highly accurate protein structure prediction with AlphaFold. Nature 2021;596(7873):583–9.
[37] Varadi M, Anyango S, Deshpande M, Nair S, Natassia C, et al. AlphaFold Protein Structure Database: massively expanding the structural coverage of protein-sequence space with high-accuracy models. Nucleic Acids Res 2022;50(D1):D439–44.
[38] Guérout-Fleury AM, Frandsen N, Stragier P. Plasmids for ectopic integration in *Bacillus subtilis*. Gene 1996;180(1–2):57–61.
[39] Zhang X, Al-Dossary A, Hussain M, Setlow P, Li J. Applications of *Bacillus subtilis* spores in biotechnology and advanced materials. Appl Environ Microbiol 2020;86(17):e01096–20.
[40] Łęga T, Weiher P, Obuchowski M, Nidzworski D. Presenting influenza A M2e antigen on recombinant spores of *Bacillus subtilis*. PLoS One 2016;11(11):e0167225.
[41] Lundstrom K. The current status of COVID-19 vaccines. Front Genome Ed 2020;2:579297.
[42] Zhang J, Fitz-James PC, Aronson AI. Cloning and characterization of a cluster of genes encoding polypeptides present in the insoluble fraction of the spore coat of *Bacillus subtilis*. J Bacteriol 1993;175(12):3757–66.
[43] Liu H, Krajcikova D, Zhang Z, Wang H, Barak I, et al. Investigating interactions of the *Bacillus subtilis* spore coat proteins CotY and CotZ using single molecule force spectroscopy. J Struct Biol 2015;192(1):14–20.
[44] Ricca E, Baccigalupi L, Isticato R. Spore-adsorption: mechanism and applications of a non-recombinant display system. Biotechnol Adv 2021;47:107693.
[45] Petrillo C, Castaldi S, Lanzilli M, Saggese A, Donadio G, et al. The temperature of growth and sporulation modulates the efficiency of spore-display in *Bacillus subtilis*. Micro Cell Fact 2020;19(1):185.
[46] https://www.uniprot.org/uniprotkb/Q08311/entry#interaction
[47] Czech A, Nowakowicz-Debek B, Łukaszewicz M, Florek M, Ossowski M, et al. Effect of fermented rapeseed meal in the mixture for growing pigs on the gastrointestinal tract, antioxidant status, and immune response. Sci Rep 2022;12(1):15764.
[48] Guo YT, Peng YC, Yen HY, Wu JC, Hou WH. Effects of probiotic supplementation on immune and inflammatory markers in athletes: a meta-analysis of randomized clinical trials. Med (Kaunas) 2022;58(9):1188.
[49] Lefevre M, Racedo SM, Denayrolles M, Ripert G, Desfougères T, et al. Safety assessment of *Bacillus subtilis* CU1 for use as a probiotic in humans. Regul Toxicol Pharm 2017;83:54–65.
[50] Amuguni H, Tzipori S. *Bacillus subtilis*: a temperature resistant and needle free delivery system of immunogens. Hum Vaccin Immunother 2012;8(7):979–86.
[51] de Souza RD, Batista MT, Luiz WB, Cavalcante RCM, Amorin JH, et al. *Bacillus subtilis* spores as vaccine adjuvants: further insights into the mechanisms of action. PLoS One 2014;9(1):e87454.
[52] Hinc K, Iwanicki A, Obuchowski M. New stable anchor protein and peptide linker suitable for successful spore surface display in *B. subtilis*. Micro Cell Fact 2013;12:22.